Transient waves along electrical transmission lines
Waves in (1+1)-spacetime

de Hoop, Adrianus; Lager, Ioan

Publication date
2019

Document Version
Final published version

Published in
13th European Conference on Antennas and Propagation, EuCAP 2019

Citation (APA)
de Hoop, A., & Lager, I. (2019). Transient waves along electrical transmission lines: Waves in (1+1)-spacetime. In *13th European Conference on Antennas and Propagation, EuCAP 2019* (pp. 1-5). Article 8740145 (13th European Conference on Antennas and Propagation, EuCAP 2019). IEEE. https://ieeexplore.ieee.org/document/8740145

Transient waves along electrical transmission lines. Waves in (1+1)-spacetime

Adrianus T. de Hoop and Ioan E. Lager
Faculty of Electrical Engineering, Mathematics and Computer Sciences, 2628 CD Delft, the Netherlands
a.t.dehoop@tudelft.nl, i.e.lager@tudelft.nl

***Abstract* — The properties of transient waves along electrical transmission lines are investigated. In particular, the excitation of the waves by impressed voltage and electric current sources is studied. Specific choices of this excitation are shown to lead to 'one-sided transmission' only. Furthermore, the reflection and transmission at a localized line fault/defect is studied. An illustrative time-domain reflectometry experiment is discussed.**

***Keywords* — reflectometry, power distribution faults.**

I. Introduction

The transient waves along electrical transmission lines (TLs) are examined as an example of wave phenomena in $(1+1)$-spacetime [1]. The goal is to derive a reflectometric strategy for determining the position *and* physical properties of localized line faults/defects. The spacetime equations are firstly constructed and are subsequently time Laplace-transformed. The expressions of the reflection and transmission coefficients at the fault for a wave excitation by means of impressed voltage and electric current sources are then derived. The reflected waves are shown to assume simple, analytic expressions for lossless cables. As an added novelty, a 'one-sided transmission' at the excitation point is obtained by matching the values of the localized impressed voltage/electric-current sources.

The described procedure finds a direct practical application in *detecting and remotely characterizing* possible faults in a wide variety of TLs, such as power lines, data-transmission lines, etc. The contribution contains a simple, but illustrative numerical experiment, convincingly demonstrating the possibilities, but also the challenges, in the case of a *time-domain reflectometry* (TDR) measurement set-up for locating and characterizing faults in megavolt DC cables.

II. Theoretical background

The electrical state quantities of the transmission line (TL) related to transient traveling wave constituents are listed in Table 1. All quantities are scalars.

A. Time-domain wave equations and constitutive relations

The coupled system of wave equations is

$$\partial_x I + \partial_t Q = I^{\text{imp}} \tag{1}$$
$$\partial_x V + \partial_t \Phi = V^{\text{imp}}. \tag{2}$$

The constitutive relations that couple the extensive wave quantities to the intensive wave quantities are

$$Q(x,t) = C\,[\delta(t) + \alpha H(t)] \overset{(t)}{*} V(x,t) \tag{3}$$

Table 1. Transient waves along electrical transmission lines.

Intensive state quantities	
I	longitudinal electric current
V	transverse (electric) voltage
Extensive state quantities	
Q	electric charge per length
Φ	magnetic flux per length
Source quantities	
I^{imp}	impressed electric current per length
V^{imp}	impressed voltage per length
Line parameters	
C	capacitance per length
G	conductance per length
L	inductance per length
R	resistance per length
$Y(t) = C\,\partial_t + G$	transverse line admittance operator per length
$Z(t) = L\,\partial_t + R$	longitudinal line impedance operator per length
Space-time coordinates	
$x \in \mathbb{R}$	position along the line
$t \in \mathbb{R}$	time coordinate
$s = \hat{\partial}_t; s \in \mathbb{R}, s > 0$	time Laplace-transform parameter

where $\alpha = G/C$ is the reciprocal of the transverse Boltzmann relaxation time [2] and

$$\Phi(x,t) = L\,[\delta(t) + \beta H(t)] \overset{(t)}{*} I(x,t) \tag{4}$$

where $\beta = R/L$ is the reciprocal of the longitudinal Boltzmann relaxation time.

B. Excitation by impressed voltages and electric currents

Using (3) and (4), the excitation of wave constituents by impressed voltages and electric currents follows from solving the system of wave equations

$$\partial_x I + Y(t)V = I^{\text{imp}} \tag{5}$$
$$\boxed{\hat{\partial}_t = s} \Rightarrow \partial_x \hat{I} + \hat{Y}\hat{V} = \hat{I}^{\text{imp}} \tag{6}$$
$$\partial_x V + Z(t)I = V^{\text{imp}} \tag{7}$$
$$\boxed{\hat{\partial}_t = s} \Rightarrow \partial_x \hat{V} + \hat{Z}\hat{I} = \hat{V}^{\text{imp}} \tag{8}$$

where

$$Y(t) = C(\partial_t + \alpha) \tag{9}$$
$$\boxed{\hat{\partial}_t = s} \Rightarrow \hat{Y}(s) = C(s + \alpha) \tag{10}$$
$$Z(t) = L(\partial_t + \beta) \tag{11}$$
$$\boxed{\hat{\partial}_t = s} \Rightarrow \hat{Z}(s) = L(s + \beta). \tag{12}$$

C. Wave equation for the electric voltage

Elimination of $\hat{I}(x,s)$ from (6) and (8) leads to the TL wave equation for the electric voltage

$$\hat{\gamma}^2\hat{V} - \partial_x^2\hat{V} = \hat{Z}\hat{I}^{\text{imp}} - \partial_x\hat{V}^{\text{imp}} \tag{13}$$

with

$$\hat{\gamma}(s) = c^{-1}\left[(s+\alpha)(s+\beta)\right]^{1/2}, \tag{14}$$

in which $c = (LC)^{-½}$ is the wavespeed.

D. Wave equation for the electric current

Elimination of $\hat{V}(x,s)$ from (6) and (8) leads to the TL wave equation for the electric current

$$\hat{\gamma}^2\hat{I} - \partial_x^2\hat{I} = \hat{Y}\hat{V}^{\text{imp}} - \partial_x\hat{I}^{\text{imp}}. \tag{15}$$

E. Green's function of the transmission-line wave equation

The time Laplace-transform domain Green's function $\hat{\Gamma}(x,s)$ of the TL wave equation is the solution to

$$\hat{\gamma}^2\hat{\Gamma} - \partial_x^2\hat{\Gamma} = \delta(x) \tag{16}$$

where $\delta(x)$ is the spatial Dirac delta distribution. To determine $\hat{\Gamma}(x,s)$, from (16) the spatial Fourier representation

$$\hat{\Gamma}(x,s) = \frac{1}{2\pi}\int_{k\in\mathbb{R}} \exp(-\mathrm{i}kx)\tilde{\Gamma}(k,s)\mathrm{d}k \tag{17}$$

is substituted. The time Laplace transform parameter s in the procedure is taken to be real and positive. The result is

$$\tilde{\Gamma} = \frac{1}{k^2+\hat{\gamma}^2} \tag{18}$$

where $\hat{\gamma}(s) > 0$ is the *real* propagation coefficient (see (14)).

To evaluate $\hat{\Gamma}$, the integrand at the right-hand side of (18) is extended into the complex k-plane. Here, the integrand has two simple poles: one at $k = -\mathrm{i}\hat{\gamma}$ and one at $k = \mathrm{i}\hat{\gamma}$. For $x < 0$, the path of integration (the real axis) is supplemented with a semi-circle in the upper half of the k-plane with arbitrarily large radius R. In view of Jordan's lemma of complex function theory, its contribution vanishes in the limit $\lim R \to \infty$. Application of Cauchy's theorem then yields

$$\hat{\Gamma} = \frac{\exp(\hat{\gamma}x)}{2\,\hat{\gamma}} \text{ for } x < 0. \tag{19}$$

A similar procedure in the lower half of the k-plane yields

$$\hat{\Gamma} = \frac{\exp(-\hat{\gamma}x)}{2\,\hat{\gamma}} \text{ for } x > 0. \tag{20}$$

Equations (19) and (20) can be taken together as

$$\hat{\Gamma}(x,s) = \frac{\exp(-\hat{\gamma}|x|)}{2\,\hat{\gamma}}. \tag{21}$$

This equation has the properties

$$\partial_x\hat{\Gamma} = -\hat{\gamma}\hat{\Gamma}(x,s)\mathrm{sgn}(x) \tag{22}$$

with $\mathrm{sgn}(x)$ being the signum function $\mathrm{sgn}(x) = \{-1, 0, 1\}$ for $\{x < 0, x = 0, x > 0\}$ and

$$\partial_x^2\hat{\Gamma} = -\delta(x) + \hat{\gamma}^2\hat{\Gamma} \tag{23}$$

since $\partial_x|x| = \mathrm{sgn}(x)$ and $\partial_x^2|x| = 2\delta(x)$. By observing that

$$\left[(s+\alpha)(s+\beta)\right]^{½} = \left[\left(s+\frac{\alpha+\beta}{2}\right)^2 - \left(\frac{\alpha-\beta}{2}\right)^2\right]^{½} \tag{24}$$

the time-domain equivalent of (21) is via [3, Formula 29.3.93]

$$\Gamma(x,t) = \frac{c}{2}\exp\left\{-\left[(\alpha+\beta)/2\right]t\right\} I_0\left[(|\beta-\alpha|/2)(t^2 - x^2/c^2)^{1/2}\right] H(t-|x|/c) \tag{25}$$

with I_0 as the modified Bessel function of the first kind.

F. Expressions for the excited voltage and electric current

Observing that for any impressed source distribution

$$\{V^{\text{imp}}, I^{\text{imp}}\}(x,t) = \{V^{\text{imp}}, I^{\text{imp}}\} \overset{(\boldsymbol{x},t)}{*} \delta(x,t) \tag{26}$$

$$\boxed{\hat{\partial}_t = s} \Rightarrow \{\hat{V}^{\text{imp}}, \hat{I}^{\text{imp}}\}(x,s) = \{\hat{V}^{\text{imp}}, \hat{I}^{\text{imp}}\} \overset{(\boldsymbol{x})}{*} \delta(x) \tag{27}$$

and introducing the traveling-wave potentials

$$A = \Gamma \overset{(\boldsymbol{x},t)}{*} I^{\text{imp}} \tag{28}$$

$$\boxed{\hat{\partial}_t = s} \Rightarrow \hat{A} = \hat{\Gamma} \overset{(\boldsymbol{x})}{*} \hat{I}^{\text{imp}} \tag{29}$$

and

$$\Psi = \Gamma \overset{(\boldsymbol{x},t)}{*} V^{\text{imp}} \tag{30}$$

$$\boxed{\hat{\partial}_t = s} \Rightarrow \hat{\Psi} = \hat{\Gamma} \overset{(\boldsymbol{x})}{*} \hat{V}^{\text{imp}} \tag{31}$$

the expression for $V(x,t)$ follows from (13) as

$$V = -\partial_x\Psi + Z(t)A \tag{32}$$

$$\boxed{\hat{\partial}_t = s} \Rightarrow \hat{V} = -\partial_x\hat{\Psi} + \hat{Z}(s)\hat{A}. \tag{33}$$

Similarly, the expression for $I(x,t)$ follows from (15) as

$$I = -\partial_x A + Y(t)\Psi \tag{34}$$

$$\boxed{\hat{\partial}_t = s} \Rightarrow \hat{I} = -\partial_x\hat{A} + \hat{Y}(s)\hat{\Psi}. \tag{35}$$

G. Wave excitation by localized impressed sources

In this section, the transient wave constituents generated by localized sources of impressed voltage and electric current are investigated.

1) Excitation by an impressed voltage source

The transient waves excited by a localized impressed voltage source follow upon substituting in (5) and (7)

$$V^{\text{imp}}(x,t) = V_0(t)\delta(x - x_V) \tag{36}$$

where $x = x_V$ is the location and $V_0(t)$ the time signature of the source, and

$$I^{\text{imp}}(x,t) = 0. \tag{37}$$

The corresponding traveling-wave potentials are

$$\Psi(x,t) = V_0(t) \overset{(t)}{*} \Gamma(x - x_V, t) \tag{38}$$

$$\boxed{\hat{\partial}_t = s} \Rightarrow \hat{\Psi}(x,s) = \hat{V}_0(s)\hat{\Gamma}(x - x_V, s) \tag{39}$$

$$A(x,t) = 0 \tag{40}$$

$$\boxed{\hat{\partial}_t = s} \Rightarrow \hat{A}(x,s) = 0. \tag{41}$$

For this kind of excitation, (6) leads to

$$\partial_x \hat{I} + \hat{Y}\hat{V} = 0 \tag{42}$$

or

$$-\hat{\gamma}(s)\mathrm{sgn}(x - x_V)\hat{I}(x,s) + \hat{Y}(s)\hat{V}(x,s) = 0 \tag{43}$$

which is rewritten as

$$\hat{I}(x,s) = \mathrm{sgn}(x - X_V)\hat{\eta}(s)\hat{V}(x,s) \tag{44}$$

where $\hat{\eta}(s) = \hat{Y}(s)/\hat{\gamma}(s)$ is the TL traveling-wave admittance. The resulting expressions for the source-excited voltage and electric current are

$$\{\hat{V}, \hat{I}\}(x,s) = \hat{V}_0(s)\left\{1, \hat{\eta}(s)\mathrm{sgn}(x - x_V)\right\}\hat{\Gamma}(x - x_V, s). \tag{45}$$

2) Excitation by an impressed electric-current source

The transient waves excited by a localized impressed electric-current source follow upon substituting in (5) and (7)

$$I^{\mathrm{imp}}(x,t) = I_0(t)\delta(x - x_I) \tag{46}$$

where $x = x_I$ is the location and $I_0(t)$ the time signature of the source, and

$$V^{\mathrm{imp}}(x,t) = 0. \tag{47}$$

The corresponding traveling-wave potentials are

$$\Psi(x,t) = 0 \tag{48}$$

$$\boxed{\hat{\partial}_t = s} \Rightarrow \hat{\Psi}(x,t) = 0 \tag{49}$$

$$A(x,t) = I_0(t) \overset{(x,t)}{*} \Gamma(x - x_I) \tag{50}$$

$$\boxed{\hat{\partial}_t = s} \Rightarrow \hat{A}(x,s) = \hat{I}(s)\hat{\Gamma}(x - x_I, s). \tag{51}$$

For this kind of excitation, (8) leads to

$$\partial_x \hat{V} + \hat{Z}\hat{I} = 0 \tag{52}$$

or

$$-\hat{\gamma}(s)\mathrm{sgn}(x - x_I)\hat{V}(x,s) + \hat{Z}(s)\hat{I}(x,s) = 0 \tag{53}$$

which is rewritten as

$$\hat{V}(x,s) = \hat{\zeta}(s)\hat{I}(x,s) \tag{54}$$

where $\hat{\zeta}(s) = \hat{Z}(s)/\hat{\gamma}(s)$ is the TL traveling-wave impedance. The resulting expressions for the source-excited electric current and voltage are

$$\{\hat{I}, \hat{V}\}(x,s) = \hat{I}_0(s)\left\{1, \hat{\zeta}(s)\mathrm{sgn}(x - x_I)\right\}\hat{\Gamma}(x - x_I, s). \tag{55}$$

III. Traveling-wave reflection and transmission at a line fault

The reflection and transmission of traveling waves at a line fault or defect is a basic issue in TDR. For analyzing such configurations, the line fault or defect is modeled as a local disturbance of the transverse line admittance operator and/or the longitudinal line impedance operator

$$\text{fault in } Y(t) = \delta Y(t)\delta(x - x_{\mathrm{F}}), \tag{56}$$

$$\text{fault in } Z(t) = \delta Z(t)\delta(x - x_{\mathrm{F}}), \tag{57}$$

in which $\delta Y(t) = \delta C\partial_t + \delta G$, $\delta Z(t) = \delta L\partial_t + \delta R$ and $x = x_{\mathrm{F}}$ is the location of the fault. Using the notations

$$[\ldots]|_-^+ = \lim_{x \downarrow x_{\mathrm{F}}}[\ldots] - \lim_{x \uparrow x_{\mathrm{F}}}[\ldots] \tag{58}$$

$$\langle\ldots\rangle_-^+ = \frac{1}{2}\left[\lim_{x \downarrow x_{\mathrm{F}}}[\ldots] + \lim_{x \uparrow x_{\mathrm{F}}}[\ldots]\right] \tag{59}$$

the presence of the fault or defect is modeled via the cross-fault electric-current or voltage, respectively, boundary conditions

$$[I]|_-^+ = \delta Y(t) \overset{(t)}{*} \langle V\rangle_-^+ \tag{60}$$

$$[V]|_-^+ = \delta Z(t) \overset{(t)}{*} \langle I\rangle_-^+ \tag{61}$$

that follow from (5) and (7) by integrating them about $x = x_{\mathrm{F}}$ under the application of the trapezoidal rule.

A. The reflectometric configuration

The analysis is carried out in the time Laplace-transform domain. In the TL section where the fault is located, an interrogating 'incident' wave $^{\mathrm{i}}$ is launched at $x = x_V$ $(x_V < x_{\mathrm{F}})$

$$\left\{\hat{V}^{\mathrm{i}}, \hat{I}^{\mathrm{i}}\right\} = \hat{V}_0(s)\left\{1, \hat{\eta}(s)\right\}\exp\left[-\hat{\gamma}(s)(x - x_V)\right] \quad \text{for } x_V < x. \tag{62}$$

At the fault, a 'reflected' wave $^{\mathrm{r}}$ is generated

$$\left\{\hat{V}^{\mathrm{r}}, \hat{I}^{\mathrm{r}}\right\} = \hat{R}(s)\hat{V}_0(s)\left\{1, -\hat{\eta}(s)\right\}\exp\left[\hat{\gamma}(s)(x - x_V - x_{\mathrm{F}})\right] \quad \text{for } x < x_{\mathrm{F}} \tag{63}$$

where $\hat{R}(s)$ is the (voltage) reflection coefficient. In the section $x > x_{\mathrm{F}}$ a 'transmitted' wave $^{\mathrm{t}}$ is generated

$$\{\hat{V}^{\mathrm{t}}, \hat{I}^{\mathrm{t}}\} = \hat{T}(s)\hat{V}_0(s)\left\{1, \hat{\eta}(s)\right\}\exp\left[-\hat{\gamma}(s)(x - x_V - x_{\mathrm{F}})\right] \quad \text{for } x_{\mathrm{F}} < x \tag{64}$$

where $\hat{T}(s)$ is the (voltage) transmission coefficient. Use of (62), (63) and (64) in (58) and (59) leads to

$$\hat{T}(s) - 1 + \hat{R}(s) + \frac{\delta\hat{Y}(s)}{2\hat{\eta}(s)}\left[\hat{T}(s) + 1 + \hat{R}(s)\right] = 0 \tag{65}$$

with $\delta\hat{Y}(s) = s\delta C + \delta G$, and

$$\hat{T}(s) - 1 - \hat{R}(s) + \frac{\delta\hat{Z}(s)\hat{\eta}(s)}{2}\left[\hat{T}(s) + 1 - \hat{R}(s)\right] = 0. \tag{66}$$

with $\delta\hat{Z}(s) = s\delta L + \delta R$. From (65) and (66) it follows that

$$\hat{R}(s) = \frac{1}{2}\left[\frac{1-\delta\hat{Y}/2\hat{\eta}}{1+\delta\hat{Y}/2\hat{\eta}} - \frac{1-\delta\hat{Z}\hat{\eta}/2}{1+\delta\hat{Z}\hat{\eta}/2}\right] \tag{67}$$

$$\hat{T}(s) = \frac{1}{2}\left[\frac{1-\delta\hat{Y}/2\hat{\eta}}{1+\delta\hat{Y}/2\hat{\eta}} + \frac{1-\delta\hat{Z}\hat{\eta}/2}{1+\delta\hat{Z}\hat{\eta}/2}\right] \tag{68}$$

Note that when $\delta Y = 0$ and $\delta Z = 0$, (67) and (68) satisfy the check $\hat{R}(s) = 0$ and $\hat{T}(s) = 1$. The reflectometric response at $x = x_V$ is then

$$\hat{V}^{\mathrm{r}}(s, x_V) = \hat{V}_0(s)\hat{R}(s)\exp\left[-2\hat{\gamma}(s)(x_{\mathrm{F}} - x_V)\right] \tag{69}$$

and is available for further processing to extract the parameters of the fault or defect.

B. Lossless line analysis

A commonly encountered situation is that when the line is lossless ($R = 0, G = 0$), implying that $\hat{\gamma} = s/c$, $\eta = (C/L)^{½}$ and $\zeta = (L/C)^{½}$, with $c = (LC)^{-½}$ being the wavespeed along the line. In that case, (67) becomes

$$\begin{aligned}\hat{R}(s) &= \frac{2\eta/\delta C}{(2\eta/\delta C + \delta G/\delta C) + s} - \frac{2/\eta\delta L}{(2/\eta\delta L + \delta R/\delta L) + s} \\ &= \frac{A_Y}{\alpha_Y + s} - \frac{A_Z}{\alpha_Z + s} = \hat{M}_Y - \hat{M}_Z.\end{aligned} \tag{70}$$

From (67) it is inferred that: when either $\delta C = 0$ or $\delta L = 0$, the corresponding term $\hat{M}_Y$ or $\hat{M}_Z$ becomes independent of s; when $\delta C = \delta L = 0$, $\hat{R}(s)$ becomes independent of s. From (69) and (70) it folows that the reflected wave in the case of a lossless line consists of constituents having a time Laplace transform of the general shape

$$\hat{V}^{\mathrm{r}}(s, x_V) = \hat{V}_0(s)\frac{A_{\mathrm{F}}\exp(-sT_{\mathrm{F}})}{(s+\alpha_{\mathrm{F}})} \text{ for } s \in \mathbb{C},\ \mathrm{Re}(s) > -\alpha_{\mathrm{F}} \tag{71}$$

for $\delta C \neq 0$ or $\delta L \neq 0$, and of the general shape

$$\hat{V}^{\mathrm{r}}(s, x_V) = \hat{V}_0(s)A_{\mathrm{F}}\exp(-sT_{\mathrm{F}}) \text{ for } s \in \mathbb{C} \tag{72}$$

for $\delta C = \delta L = 0$, where T_{F} is the two-way travel time from the line's access point to the location of the fault, and back.

C. Localized combined impressed voltage/electric-current source excitation – one-sided excitation

The transient waves excited by a localized combined impressed voltage/electric-current source follow upon substituting in (5) and (7)

$$V^{\mathrm{imp}}(x,t) = V_0(t)\delta(x - x_{VI}) \tag{73}$$

$$\boxed{\hat{\partial}_t = s} \Rightarrow \hat{V}^{\mathrm{imp}}(x,s) = \hat{V}_0(s)\delta(x - x_{VI}) \tag{74}$$

$$I^{\mathrm{imp}}(x,t) = I_0(t)\delta(x - x_{VI}) \tag{75}$$

$$\boxed{\hat{\partial}_t = s} \Rightarrow \hat{I}^{\mathrm{imp}}(x,s) = \hat{I}_0(s)\delta(x - x_{VI}) \tag{76}$$

where $x = x_{VI}$ is the location of the source and $\{V_0(t), I_0(t)\}$ are its time signatures. The corresponding wave potentials are

$$\Psi(x,t) = V_0(t) \overset{(t)}{*} \Gamma(x - x_{VI}, t) \tag{77}$$

$$\boxed{\hat{\partial}_t = s} \Rightarrow \hat{\Psi}(x,s) = \hat{V}_0(s)\hat{\Gamma}(x - x_{VI}, s) \tag{78}$$

$$A(x,t) = I_0(t) \overset{(t)}{*} \Gamma(x - x_{VI}, t) \tag{79}$$

$$\boxed{\hat{\partial}_t = s} \Rightarrow \hat{A}(x,s) = \hat{I}_0(s)\hat{\Gamma}(x - x_{VI}, s). \tag{80}$$

From (45) and (55) the resulting expressions for the source-excited voltage and electric current are

$$\begin{aligned}\left\{\hat{V}, \hat{I}(x,s)\right\} &= \hat{V}_0(s)\left\{1, \hat{\eta}(s)\mathrm{sgn}(x - x_{VI})\right\}\hat{\Gamma}(x - x_{VI}, s) \\ &+ \hat{I}_0(s)\left\{\hat{\zeta}(s)\mathrm{sgn}(x - x_{VI}), 1\right\}\hat{\Gamma}(x - x_{VI}, s).\end{aligned} \tag{81}$$

For $\hat{V}_0(s) = \hat{I}_0(s)\hat{\zeta}(s)$ (81) yields

$$\{\hat{V}, \hat{I}\}(x,s) = 0 \text{ for } x < x_{VI} \tag{82}$$

whereas for $\hat{V}_0(s)\hat{\eta}(s) = -\hat{I}_0(s)$ (81) yields

$$\{\hat{V}, \hat{I}\}(x,s) = 0 \text{ for } x > x_{VI} \tag{83}$$

namely one-sided excitation results.

IV. The Echogram as a Diagnostic Tool

Monitoring the operation of large grid systems for electric power transmission and distribution [4], [5] presents testing challenges, one of them being detecting, locating and characterizing faults in kilovolt or megavolt DC cables. Presently, there is a vast bibliography on fault detection schemes for overhead TLs and, more recently, for cables, with traveling-wave based fault location being widely credited as the path to follow. Most strategies use a TDR measurement set-up, in which a pulse with a suitable waveform is injected at an access point, and the time-of-arrival of the reflected wave measured at the same point gives an indication of the fault's location. The accuracy of TDR methods hinges on the knowledge of the line parameters [6] and the detection of the incoming pulse [8], [9].

In this section we shall demonstrate how information about the (physical) nature of the fault can also be extracted from the time signature of the reflected pulse. The cable under investigation is modeled as a uniform section of *lossless* TL with an access point that is activated by impressing a voltage pulse (or a pulsed electric current surge). The system's response is monitored at the same point via a tester displaying the exciting voltage and the response(s).

A. Analytic model pulse shapes

As the basic pulse shape for modeling analytically the excitation of the cable under test we take the *exponential pulse*

$$V_0(t) = A_0\exp(-\alpha_0 t)H(t) \tag{84}$$

where A_0 is the amplitude, and the pulse time width $t_{\mathrm{w},0}$ – the latter is related to the time decay coefficient α_0 via $t_{\mathrm{w},0} = \alpha_0^{-1}$. The pulse's time Laplace transform is

$$\hat{V}_0(s) = \frac{A_0}{s+\alpha_0} \text{ for } s \in \mathbb{C},\ \mathrm{Re}(s) > -\alpha_0. \tag{85}$$

B. *Reflector parameters extraction*

For lossless cables, (71) implies that the reflection at a cable fault for an excitation of the type (85) will also have an exponential pulse shape. The reflected wave constituent has then a time Laplace transform of the general shape

$$\hat{V}^{\mathrm{r}}(s, x_V) = \frac{A\exp(-sT_{\mathrm{F}})}{(s+\alpha_0)(s+\alpha_{\mathrm{F}})} \quad \text{for } s \in \mathbb{C},\ \mathrm{Re}(s) > -\min(\alpha_0, \alpha_{\mathrm{F}}) \tag{86}$$

that yields the time-domain reflected wave

$$V^{\mathrm{r}}(t) = \frac{A}{\alpha_{\mathrm{F}} - \alpha_0}\left[\exp(-\alpha_0 t') - \exp(-\alpha_{\mathrm{F}} t')\right] H(t') \quad \text{for } \alpha_0 \neq \alpha_{\mathrm{F}} \tag{87}$$

$$V^{\mathrm{r}}(t) = A\, t' \exp(-\alpha t') H(t') \text{ for } \alpha_0 = \alpha_{\mathrm{F}} = \alpha \tag{88}$$

with $t' = t - T_{\mathrm{F}}$. This type of signatures are denoted as *exponential doublet pulses* (`Exp2-pulse`). By following a similar reasoning, (71) will yield a time-retarded, scaled copy of the excitation pulse as reflected wave.

At this point it is noted that, in general, the extraction of the desired parameters from the reflector's TD reflection function as it occurs in the pertaining reflected wave requires a deconvolution of this signal with the excitation, through the application of signal processing deconvolution algorithms. Some of the parameters can, however, be directly obtained from the echogram itself. This will be elucidated for the case when the excitation takes place with the pulse in (84). In view of editorial space restrictions, the more general situation when δC or δL are nonzero is elaborated upon (the cases when either one of, or both δC or δL are zero can be dealt with in a similar manner). Let us consider one of such constituents

$$V(t) = \frac{A}{\alpha_{\mathrm{F}} - \alpha_0}[\exp(-\alpha_0 t) - \exp(-\alpha_{\mathrm{F}} t)]H(t) \tag{89}$$

with $\alpha_0 \neq \alpha_1$. In the echogram, this pulse shows a peak value V^{peak} at the pulse rise time t_{r}. By taking $\partial_t V(t) = 0$ for $t = t_{\mathrm{r}}$, this peak value is $V^{\mathrm{peak}} = (A/\alpha_{\mathrm{F}})\exp(-\alpha_0 t_{\mathrm{r}})$. Carrying out the sensing experiment with two different values of α_0 and extracting from the echograms the values of V_0, V^{peak} and t_{r}, two relations between A and α_{F} follow, from which the values for the reflector under consideration can be obtained.

C. *Illustrative signatures for the three basic configurations*

Some illustrative signatures are hereafter given. The reflection functions associated with the reflection due to faults are shown in Fig. 1. The superposition of two `Exp2-pulse`-s is visible. The echograms demonstrate the sharp change at the reflected wave's arrival time T_{F}, this allowing an accurate determination of the distance to the termination. However, the amplitude of the reflected wave is quite smaller and, moreover, drops as the fault's contrast with respect to the line's traveling-wave admittance $\hat{\eta}$ and impedance $\hat{\zeta}$, respectively, decreases. This may affect the ability to accurately determine the distance to the fault in the cases when noisy signatures are received. This amplitude reduction must also be accounted for in the case of algorithms for reconstructing the fault's parameters.

REFERENCES

[1] A. T. de Hoop, "Electromagnetic field theory in (N+1)-space-time: A modern time-domain tensor/array introduction," *Proc. IEEE*, vol. 101, no. 2, pp. 434–450, Feb. 2013.

[2] L. Boltzmann, "Zur Theorie der elastischen Nachwirkung," *Poggendorff's Annalen der Physik und Chemie*, vol. 7, pp. 624–654, 1876.

[3] M. Abramowitz and I. A. Stegun, *Handbook of Mathematical Functions*, Mineola, NY: Dover Publications, 1968.

[4] J. Kumagai, "The U.S. may finally get a unified power grid," *IEEE Spectrum*, vol. , no. 1, pp. 31-32, Jan. 2016.

[5] Y. Ohki and S. Yasufuku, "The world's first long-distance 500kV-XLPE cable line, Part 2: Joints and after-installation test," *IEEE Elect. Insul. Mag.* vol. 18, no. 3, pp. 57–58, May/Jun. 2002.

[6] G. B. Ancell and N. C. Pahalawaththa, "Effects of frequency dependence and line parameters on single ended travelling wave based fault location schemes," *IEE Proc.-C*, vol. 139, no. 4, pp. 332–342, Jul. 1992.

[7] N. I. Elkalashy, N. A. Sabiha, and M. Lehtonen, "Earth fault distance estimation using active traveling waves in energized-compensated MV networks," *IEEE Trans. Power Del.*, vol. 30, no. 2, pp. 836–843, Apr. 2015.

[8] F. H. Magnago and A. Abur, "Fault location using wavelets," *IEEE Trans. Power Del.*, vol. 13, no. 4, pp. 1475–1480, Oct. 1998.

[9] Z.-L. Gaing, "Wavelet-based neural network for power disturbance recognition and classification," *IEEE Trans. Power Del.*, vol. 19, no. 4, pp. 1560–1568, Oct. 2004.

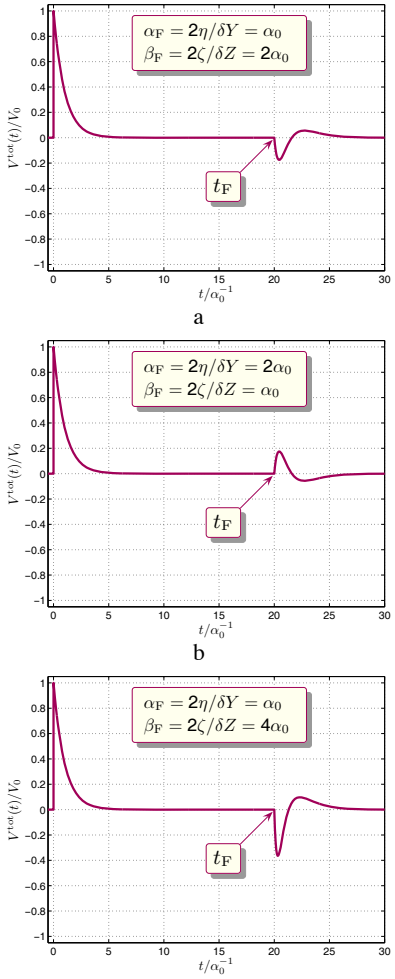

Fig. 1. Echograms for faults. $T_Y = 2\,cx_{\mathrm{F}}$ is the two-way travel time from the access point of the cable to the position of the fault and back.